Preprints of the 19th World Congress
The International Federation of Automatic Control
Cape Town, South Africa. August 24-29, 2014

Dynamic Modeling and Image-based Adaptive Visual Servoing of Cable-driven Soft Robotic Manipulator

Hesheng Wang* Weidong Chen* Chao Wang*, Xiaozhou Wang, and Rolf Pfeifer***

* *Key Laboratory of System Control and Information Processing, Ministry of Education of China, Department of Automation,* Shanghai *Jiao Tong University, Shanghai 200240, China (Tel: 86-21-34204302; e-mail: wdchen@sjtu.edu.cn).*

** *Shanghai Chest Hospital, Shanghai Jiao Tong University, Shanghai, china.,*

Abstract: This paper focus on dynamic visual seroving of a cable-driven soft robotic manipulator system. The soft robotic manipulator has no rigid structure. Based on Lagrange mechanics, kinetic energy, elastic potential energy and gravitational potential energy of each segment are analyzed, thus general dynamic equation of the soft robotic manipulator is obtained. On this basis, a depth-independent image Jacobian matrix is presented and an image-based visual servo controller is designed. Applied by adaptive algorithm, the controller could estimate unknown 3D feature positions online, and Lyapunov method is involved to prove the stability of the system. Experiments are conducted to demonstrate reasonableness and validity of dynamic model of the soft robotic manipulator and image-based adaptive visual servo controller.

1. INTRODUCTION

The soft robot is inspired by nature. Through the observation and research on the mammalian tongue, elephant nose, octopus tentacles, researchers found that biological could change their shapes and sizes to suit different environments and tasks. These physiology and movement mechanisms are used for design and development of robots. Different from traditional rigid robots, discrete high-redundant robots and hard continuum robot, soft robots are usually made of elastic material, with an infinite number of degrees of freedom, and thus has an advantage of safety and flexibility over other types of robots (Trivedi et al). It can perform complex motion in crowded and restricted environment, which makes it particularly suitable for rescue task (Wolf et al), minimally invasive surgery (Simaan et al) or other fields. Although soft robot exhibits many advantages, there are still some technical problems, limiting its practical application. Two most prominent points are establishing accurate kinematic and dynamic models, and achieving precise motion control.

Kinematics and dynamics models are important for trajectory planning and motion control of a soft robot. In dynamic modeling, Webster, et. al proposed mechanics modeling methods and energy minimization modeling methods based on the theory of elasticity and Cosserat rod. However none of the above methods were specifically addressed and compared. Tatlicioglu et al established a dynamic model for a continuous planar manipulator, and added gravitational potential energy term and elastic potential energy term in this model so that the model is consistent with the actual behaviour of the robot arm. However, the model does not apply to three-dimensional space motion control. Trivedi et. al Established a model for pneumatic manipulator based on Cosserat rod theory by taking the nonlinearity in material, distributed load weight and other factors into account. However Cosserat rod theory requires strict conditions that not all soft robot can meet. Zheng et al built a three-dimensional dynamic model with four vertical and four horizontal muscles by presenting muscles by distributed elastic force and the damping force. The method based on the force balance often contains many equations, which increases the difficulty of calculations.

Because it is difficult to establish precise kinematic and dynamic models, information provided by the sensors are necessary in order to realize the soft robot's motion control. While visual information is undoubtedly the most common used. In visual servo, an important issue need to be addressed is to calculate the depths of the feature points which is unknown in uncalibrated case. At present, stereo vision method (Deng et al) and homography method (Hu et al), are widely used to estimate the image Jacobian matrix (Hosada et al) or depth. In our earlier work (Liu et al, Wang et al (2008, 2012)), visual servoing method is proposed based on the depth-independent image Jacobian. Currently, there is few literature about using visual servo methods to achieve accurate position control of soft robot. We (Wang et al (2013)) developed the first visual servo controller for soft robot. However, this method is based on kinematics only. Neglecting dynamics will decrease the performance of the system or even make the system unstable.

This paper designs a cable driven soft robot manipulator system. Lagrange method is used to analyze the kinetic and potential energy, then the dynamic model is established. On this basis, we propose an adaptive image-based visual servo controller. The proposed controller can achieve precise position control of the soft robot when the feature point position is unknown. Lyapunov method is applied to prove the asymptotic stability of the system. Finally, the experiments conducted on a soft robot manipulator demonstrate the effectiveness of dynamics-based adaptive visual servo controller.

2. DYNAMIC MODELING OF THE SOFT ROBOT MANIPULATOR

As shown in Fig.1, the soft robotic manipulator developed in our laboratory is made of silicone rubber and has no rigid structure inside. Inspired by octopus tentacle, the current prototype is cone-shaped, and 300mm in length, 8mm and 30mm in diameters of the tip plane and the base plane respectively. An endoscope camera is embedded along the center axis to provide visual feedback for the robot. 4 cables are uniform distributed near the outer surface of the manipulator with 90°respect to each other. One side of the cables is tied to a small ring embedded in the tip, and the other side is coined around pulleys.

Let q be the length variables of 4 cables in the actuation space and p be the position and orientation of the end-effector in the task space. The configuration of the soft robotic manipulator is expressed by the virtual joint variables ϕ,θ,r . Specifically, ϕ denotes the angle between the bending plane and the positive direction of x axis, θ and r denote the curvature angle and curvature radius of the bending plane respectively.

The soft robotic manipulator is cone-shaped, thus the central axis varies in curvature according to the radius of transverse section. To simplify the solving procedure, the piecewise constant curvature hypothesis is introduced, that is, evenly dividing the whole body of the soft robotic manipulator into n segments, and each segment can be treated as a cylinder that the radius of the upper section is equal to the one of the lower section. Fig.2 illustrates the i-th segment of the soft robotic manipulator.

The radius of transverse section of the soft robot manipulator is variant. However when the number of segments tends to infinity, each segment can be approximated as a thin disk with the constant radius for the cross-section. As the short dashed line shows in Figure 3. Let R_1 and R_2 be the radii of the base plane and tip plane, where $R_2 > R_1$, the radius of transverse section of the i-th segment R_i can be represented as:

$$R_i = R_2 + \frac{i}{n}\left(R_1 - R_2\right) \tag{1}$$

Let L be the initial length of 4 cables and q_1,q_2,q_3,q_4 be the length variables of 4 cables The virtual joint variables of the i-th segment ϕ_i,θ_i can be written as following form (For detail analysis of Kinematics, please refer to our earlier work Wang et al (2013):

$$\phi_i = \tan^{-1}\frac{q_4 - q_2}{q_3 - q_1} \tag{2}$$

$$\theta_i = \frac{\sqrt{\left(q_3 - q_1\right)^2 + \left(q_4 - q_2\right)^2}}{2nR_i} \tag{3}$$

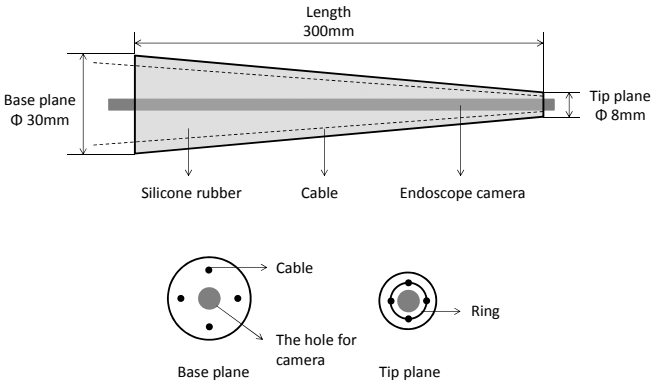

Fig.1 The cable-driven soft robotic manipulator.

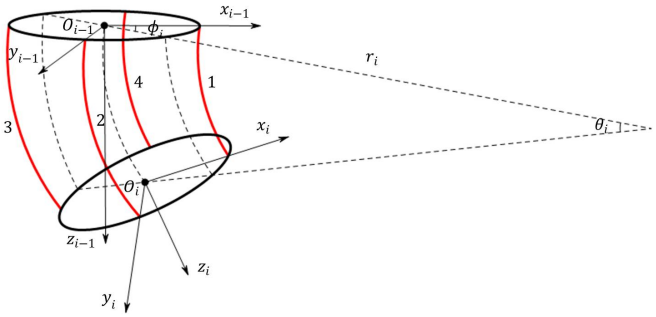

Fig.2 The i-th segment of the soft robotic manipulator.

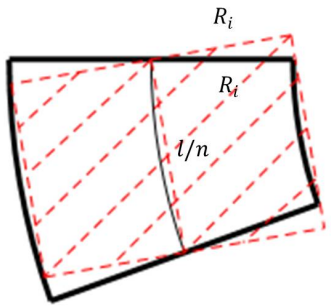

Fig.3 i-th segment which is treated as a thin disk

The centroid coordinates of the i-th segment in the base frame could be calculated by Kinematics

$$x_i = \cos\phi\frac{l}{n}\left[\sin\left(\frac{\theta_1}{2}\right) + \sin\left(\theta_1 + \frac{\theta_2}{2}\right)\cdots + \sin\left(\theta_1 + \theta_2 + \cdots + \frac{\theta_i}{2}\right)\right]$$

$$y_i = \sin\phi\frac{l}{n}\left[\sin\left(\frac{\theta_1}{2}\right) + \sin\left(\theta_1 + \frac{\theta_2}{2}\right)\cdots + \sin\left(\theta_1 + \theta_2 + \cdots + \frac{\theta_i}{2}\right)\right]$$

$$z_i = \frac{l}{n}\left[\cos\left(\frac{\theta_1}{2}\right) + \cos\left(\theta_1 + \frac{\theta_2}{2}\right) + \cdots + \cos\left(\theta_1 + \theta_2 + \cdots + \frac{\theta_i}{2}\right)\right] \tag{4}$$

$\left(x_i, y_i, z_i\right)$ could be transformed as:

$$\begin{aligned} x_i &= l\cos\phi f_1 \\ y_i &= l\sin\phi f_1 \\ z_i &= l f_2 \end{aligned} \tag{5}$$

where

$$l = L - \frac{q_1 + q_2 + q_3 + q_4}{4} \tag{6}$$

$$f_1 = \frac{\left(1 + c_2\frac{i}{n}\right)\sin\left[c_1 \ln\left(1 + c_2\frac{i}{n}\right)\right] - c_1\left(1 + c_2\frac{i}{n}\right)\cos\left[c_1 \ln\left(1 + c_2\frac{i}{n}\right)\right] + c_1}{\left(1 + c_1^2\right)c_2} \tag{7}$$

$$f_2 = \frac{c_1\left(1 + c_2\frac{i}{n}\right)\sin\left[c_1 \ln\left(1 + c_2\frac{i}{n}\right)\right] + \left(1 + c_2\frac{i}{n}\right)\cos\left[c_1 \ln\left(1 + c_2\frac{i}{n}\right)\right] - 1}{\left(1 + c_1^2\right)c_2} \tag{8}$$

$$c_1 = \frac{\sqrt{\left(q_3 - q_1\right)^2 + \left(q_4 - q_2\right)^2}}{2\left(R_1 - R_2\right)} \tag{9}$$

$$c_2 = \frac{R_1 - R_2}{R_2} \tag{10}$$

Let ρ denotes the current density of the soft robot manipulator, l denotes the current length of the center arc. Then the total mass of the soft robot arm can be presented as follows cumulative form, and could be converted to integral form as

$$\begin{aligned} M &= \sum_{k=1}^{n} \rho\pi R_i^2 \frac{l}{n} \\ &= \int_0^1 \rho l\pi \left[R_2 + \left(R_1 - R_2\right)\delta\right]^2 d\delta \\ &= \rho l\pi \left[R_2^2 + R_2\left(R_1 - R_2\right) + \frac{1}{3}\left(R_1 - R_2\right)^2\right] \end{aligned} \tag{11}$$

where

$$\rho = \frac{M}{\pi l\left[R_2^2 + R_2\left(R_1 - R_2\right) + \frac{1}{3}\left(R_1 - R_2\right)^2\right]} \tag{12}$$

The mass of the i-th segment could be obtained:

$$\begin{aligned} m_i &= \rho\pi R_i^2 \frac{l}{n} \\ &= \frac{M\left[R_2 + \frac{i}{n}\left(R_1 - R_2\right)\right]^2}{n\left[R_2^2 + R_2\left(R_1 - R_2\right) + \frac{1}{3}\left(R_1 - R_2\right)^2\right]} \end{aligned} \tag{13}$$

For the i-th segment, the cross-sectional radius of the disk R_i is much larger than the height of the disc $\frac{l}{n}$, and the moment of inertia J_i can be expressed as:

$$\begin{aligned} J_i &= \frac{1}{4} m_i R_i^2 \\ &= \frac{M\left[R_2 + \frac{i}{n}\left(R_1 - R_2\right)\right]^4}{4n\left[R_2^2 + R_2\left(R_1 - R_2\right) + \frac{1}{3}\left(R_1 - R_2\right)^2\right]} \end{aligned} \tag{14}$$

The rotation angel β_i of the i-th segment is

$$\begin{aligned} \beta_i &= \theta_1 + \theta_2 + \cdots + \frac{\theta_i}{2} \\ &= \frac{\sqrt{\left(q_3 - q_1\right)^2 + \left(q_4 - q_2\right)^2}}{2\left(R_1 - R_2\right)} \ln\left(1 + \frac{R_1 - R_2}{R_2}\frac{i}{n}\right) \end{aligned} \tag{15}$$

The kinetic energy of the i-th segment t_i is generated due to the translational and rotational motion of the disc and it could be written as follows

$$t_i = \frac{1}{2} m_i \left(\dot{x}_i^2 + \dot{y}_i^2 + \dot{z}_i^2\right) + \frac{1}{2} J_i \dot{\beta}_i^2 \tag{16}$$

For the soft robot manipulator, its potential energy contains not only the gravitational potential energy, but also the elastic potential energy. It can be interpreted as the energy reserved when the soft robot manipulator is in a compressed or stretched state due to the four cables' length change. By the definition, the elastic potential energy of the i-th segment u_{ei} can be expressed as:

$$u_{ei} = \frac{1}{2} E \frac{\left(\frac{q}{n}\right)^2}{\frac{L}{n}} \pi R_i^2 = \frac{Eq^2\pi R_2^2}{2nL}\left(1 + c_2\frac{i}{n}\right)^2 \tag{17}$$

Where E is the Young's modulus, and its value depends on the material characteristics.

The gravitational potential energy u_{gi} of the i-th segment can be expressed as

$$\begin{aligned} u_{gi} &= m_i g z_i \\ &= \frac{Mg\left(1 + c_2\frac{i}{n}\right)^2}{n\left(1 + c_2 + \frac{1}{3}c_2^2\right)}\left(L - q\right) \\ &\quad \frac{\left(1 + c_2\frac{i}{n}\right)\cos\left[c_1 \ln\left(1 + c_2\frac{i}{n}\right)\right] + c_1\left(1 + c_2\frac{i}{n}\right)\sin\left[c_1 \ln\left(1 + c_2\frac{i}{n}\right)\right] - 1}{\left(1 + c_1^2\right)c_2} \end{aligned} \tag{18}$$

The total kinetic energy T and potential energy U of the soft robot manipulator could be calculated by integration of the kinetic energy t_i, the elastic potential energy u_{ei} and gravitational potential energy u_{gi} of the i-th segment. Then, substitute them into the Lagrange equation:

$$\frac{d}{dt}\left(\frac{\partial T}{\partial \dot{q}_i}\right) - \frac{\partial T}{\partial q_i} + \frac{\partial U}{\partial q_i} = \tau_i \tag{19}$$

where $i = 1, 2, 3, 4$, q_i is length changes of the 4 cables. $\dot{q}_i$ is the rate of change of the length of the 4 cables, τ is the input forces to pull 4 cables. The equation (19) could

eventually be transformed into the general dynamics equation with the following form:

$$H\left(q(t)\right)\ddot{q}(t)+\left\{\frac{1}{2}\dot{H}\left(q(t)\right)+C\left(q(t),\dot{q}(t)\right)\right\}\dot{q}(t)+G\left(q(t)\right)=\tau(t) \tag{20}$$

where $H\left(q(t)\right)$ is the positive-definite inertial matrix. $C\left(q(t),\dot{q}(t)\right)$ is a skew-symmetric matrix. These first three terms in equation (20) represent the inertial force, the Colioris and centrifugal forces, and the gravitational force respectively.

3. VISUAL SERVOING OF SOFT ROBOT MANIPULAOTR

An eye-in-hand system of the soft robotic manipulator is set up (Fig.4). Let ${}^{e}T_{b}\left(q(t)\right)$ be the homogeneous transformation matrix of the base frame with respect to the end-effector frame, it could be calculated by direct kinematics of the soft robotic manipulator and has relation to the length variables of 4 cables $q(t)$.

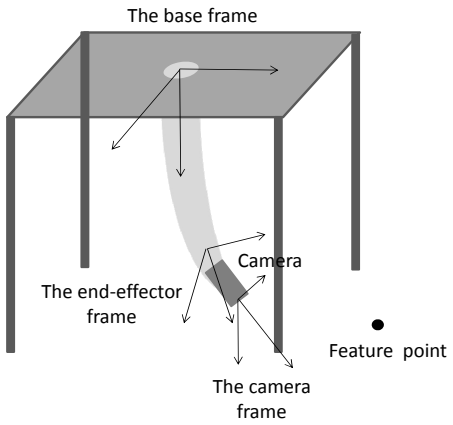

Fig.4 The eye-in-hand system of the soft robotic manipulator.

Let ${}^{b}x$ be 3D coordinate of a feature point in the base frame. For a feature point with uncalibrated case, ${}^{b}x$ is unknown.

Assume that the endoscope camera is a perspective projection camera. Denote the 2D coordinate of the feature point on the image plane by $y(q(t))$, therefore the projection of the feature point on the image plane can be written in homogeneous coordinate forms:

$$y(q(t))=\frac{1}{z(q(t))}P\,{}^{e}T_{b}\left(q(t)\right)\begin{bmatrix}{}^{b}x\\1\end{bmatrix} \tag{21}$$

where $z(q(t))$ is the depth of the feature point respect to the camera frame and

$$z(q(t))=m_3^{T}\,{}^{e}T_{b}\left(q(t)\right)\begin{bmatrix}{}^{b}x\\1\end{bmatrix} \tag{22}$$

where P is a sub-matrix contain only the first two rows vector of the perspective projection matrix M.

By differentiating Eq. (21) - (22), following relationship could be built up:

$$\dot{y}(q(t))=\frac{1}{z(q(t))}A(y(t),q(t))\begin{bmatrix}v(t)\\w(t)\end{bmatrix} \tag{23}$$

$$\dot{z}(q(t))=b(q(t))\begin{bmatrix}v(t)\\w(t)\end{bmatrix} \tag{24}$$

where $A(y(t),q(t))$ is depth-independent image Jacobian matrix.

Based on the method of PD feedback control with gravity compensation, a kinematics-based visual servo controller is designed as follows:

$$\begin{aligned}\tau(t)=&-K_1\dot{q}(t)-J^{T}\left(q(t)\right)\hat{A}^{T}\left(y(t),q(t)\right)K_2\Delta y(t)\\&+G\left(q(t)\right)-\frac{1}{2}J^{T}\left(q(t)\right)\hat{b}^{T}\left(q(t)\right)\Delta y^{T}(t)K_2\Delta y(t)\end{aligned} \tag{25}$$

Where $\Delta y(t)=y(t)-y_d$, $y(t)$ and y_d are the current position and desired position of the feature point on the image plane respectively. $\hat{A}^{T}(y(t),q(t))$ and $\hat{b}^{T}(q(t))$ mean that they are estimated value and can be computed by the estimate value of the position of the feature point in the base frame ${}^{b}\hat{x}(t)$.

To estimated the unknown position ${}^{b}x$, following adaptive algorithm is adopted similar to Slotine-Li algorithm:

$${}^{b}\dot{\hat{x}}(t)=-\Gamma^{-1}Y^{T}\left(y(t),q(t)\right)\dot{q}(t) \tag{26}$$

Where Γ is a positive definite gain matrix.

Applying the image-based visual servo controller in Eq. (25) and adaptive algorithm in Eq. (26), it can be proved that the position error of the feature point on the image plane will be convergent to zero when time approaches to the infinity:

$$\lim_{t\to\infty}\Delta y(t)=0 \tag{27}$$

To prove the conclusion above, a Lyapunov-like function is defined as follows:

$$\begin{aligned}V(t)=&\frac{1}{2}\dot{q}^{T}(t)H\left(q(t)\right)\dot{q}(t)+\frac{1}{2}\Delta y^{T}(t)K_2z\left(q(t)\right)\Delta y(t)\\&+\frac{1}{2}\Delta\,{}^{b}x^{T}(t)\Gamma\Delta\,{}^{b}x(t)\end{aligned} \tag{28}$$

Differentiating the function *V(t)* results in

$$\dot{V}(t)=\dot{q}^T(t)H(q(t))\ddot{q}(t)+\frac{1}{2}\dot{q}^T(t)\dot{H}(q(t))\dot{q}(t)$$
$$+\Delta y^T(t)K_2 z(q(t))\Delta\dot{y}(t)+\frac{1}{2}\Delta y^T(t)K_2\dot{z}(q(t))\Delta y(t)$$
$$+\Delta^b x^T(t)\Gamma\Delta^b\dot{x}(t) \qquad (29)$$

By substituting the controller (25) in the system dynamic equation (20) and Multiplying the $\dot{\mathbf{q}}^T(t)$ to both side of this equation, the following equations could be obtained:

$$\dot{q}^T(t)H(q(t))\ddot{q}(t)+\frac{1}{2}\dot{q}^T(t)\dot{H}(q(t))\dot{q}(t)$$
$$=-\dot{q}^T(t)K_1\dot{q}(t)-\dot{q}^T(t)J^T(q(t))A^T(y(t),q(t))K_2\Delta y(t)$$
$$-\frac{1}{2}\dot{q}^T(t)J^T(q(t))b^T(q(t))\Delta y^T(t)K_2\Delta y(t)$$
$$+\dot{q}^T(t)Y(y(t),q(t))\Delta^b x(t) \qquad (30)$$

Where $Y(y(t),q(t))$ is a regression matrix independent of unknown position ${}^b x$. $\Delta^b x(t)\left(={}^b\hat{x}(t)-{}^b x\right)$ indicates the 3D position error of the feature point in the base frame.

From equations（23）, （24）and（26）, we know:

$$\dot{q}^T(t)J^T(q(t))A^T(y(t),q(t))=z(q(t))\Delta\dot{y}^T(t) \qquad (31)$$

$$\dot{q}^T(t)J^T(q(t))b^T(q(t))=\dot{z}^T(q(t)) \qquad (32)$$

$$\Delta^b x^T(t)\Gamma\Delta^b\dot{x}(t)=-\Delta^b x^T(t)Y^T(y(t),q(t))\dot{q}(t) \qquad (33)$$

By combining above euquations, $\dot{V}(t)$ could be simplied as:

$$\dot{V}(t)=-\dot{q}^T(t)K_1\dot{q}(t) \qquad (34)$$

It could be proved that $\dot{V}(t)$ is uniformly continuous. From Barbalat's Lemma, the following convergence could be conluded:

$$\lim_{t\to\infty}\dot{q}(t)=0 \qquad (35)$$

By considering the closed-loop system dynamic equation (30), and using a similar proof to (Wang et al 2008), it could be proved that in the invariant set the image error will be converged to zero.

4. EXPERIMENTS

The soft robot manipulator experimental platform is shown in Fig.5. It consists of a flexible arm body and external driver mechanism. The external driver mechanism is composed of a bracket, a servo control board, four motors and four pulleys.

As shown in Figure 6, the left part shows the projection of feature points on the image plane and the right part is the real environment contains this feature point. The objective of visual servoing is to drivers the image feature point from the current position (green circle mark) to the desired position (red circle) by controlling the movement of the soft robot manipulator. When the green circle in the figure coincides with the red circle, visual servoing task is completed. Initially, the feature point coordinates in the base frame is unknown, an initial roughly guess is necessary. This parameter will be estimated by the adaptive algorithm on-line. The gains for controller are selected as: $K_1=1.0\times10^{-10}$, $K_2=3.0\times10^{-6}$ and $\Gamma=100$.

Fig.7 shows the image trajectory of the feature point and Fig.8 plots the image errors between current position and desired position. These figures shows the image feature point can quickly converge to the desired location, which verified the validity of the adaptive visual servo controller. Please note there are chattering effects on these figure, how to deal with these will be one of our future work.

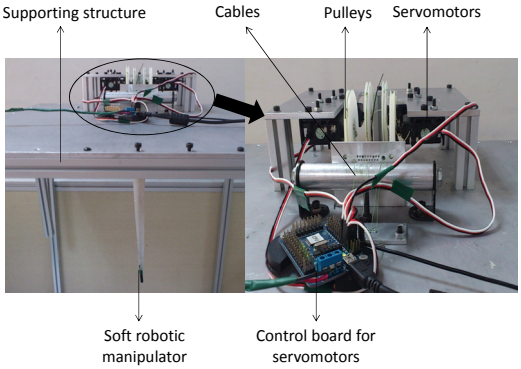

Fig.5 The soft robotic manipulator system.

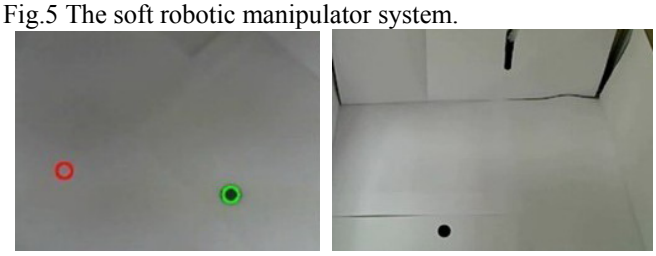

Fig.6 The feature point on image plane and real environment

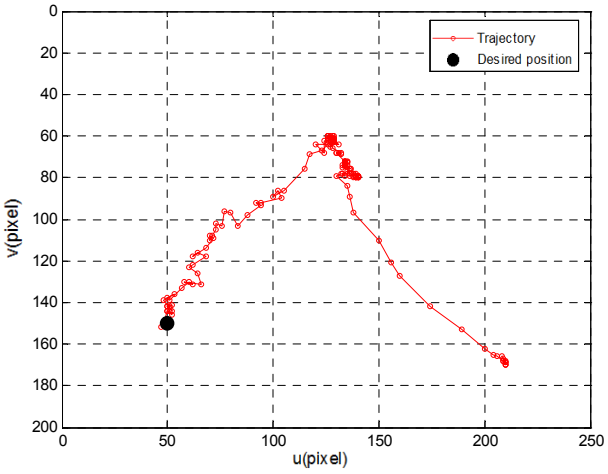

Fig.7 The trajectory of the feature point on the image plane

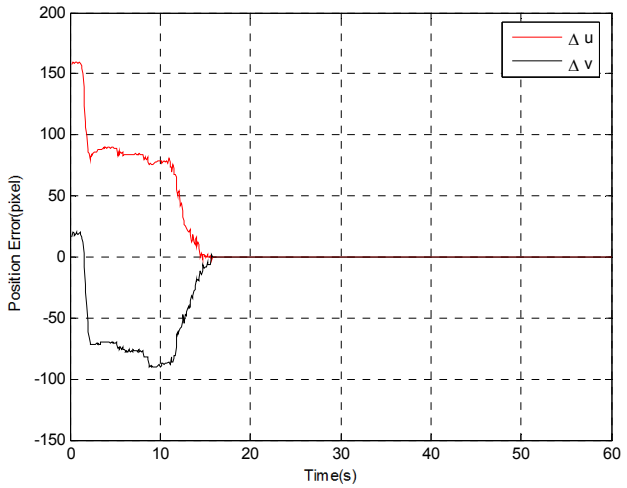

Fig.8 The errors between current position and desired position of the feature point

5. CONCLUSIONS

In this paper, a dynamic model of soft robot manipulator is derived based on Lagrangian mechanics with Piecewise constant curvature assumptions. On this basis, the depth independent image Jacobian matrix is adopted for visual servo controller design. To achieve precise position control of the end-effector of the soft robot, adaptive algorithm is developed to estimate the feature points parameters on-line. Lyapunov method is involved to prove the stability property of the system. Finally, the effective of the proposed adaptive visual servo controller is demonstrated based on dynamic visual servo experiments.

ACKNOWLEDGMENT

This work was supported in part by Shanghai Municipal Natural Science Foundation under Grant 11ZR1418400, in part by Shanghai Rising-Star Program under Grant 14QA1402500, in part by the Natural Science Foundation of China under Grant 61105095, in part by China Domestic Research Project for the International Thermonuclear Experimental Reactor (ITER) under Grant 2012GB102001 and 2012GB102008, in part by Medical Engineering Project of Shanghai Jiao Tong University under Grant YG2011ZD08.

REFERENCES

Deng L., Janabi-Sharifi F., and Wilson W. J. (2002). Stability and robustness of visual servoing methods. In: Prof. of IEEE Int. Conf. on Robotics and Automation, pp. 1604 – 1609, Washington, DC , USA.

Hu G., Mackunis W., Gans N., Dixon W. E., Chen J., Behal A., Dawson D.M. (2009). Homography-Based Visual Servo Control with Imperfect Camera Calibration. IEEE Trans. on Automatic Control, Vol. 54, No. 6, pp. 1318-1324.

Hosada K. and Asada M. (1994). Versatile visual servoing without knowledge of true Jacobain. In: Proc. of IEEE/RSJ Int. Conf. on Intelligent Robots and Systems, pp. 186-191, Munich, Germany.

Liu Y. H., Wang H., Wang C. and Lam K. (2006). Uncalibrated visual servoing of robots using a depth-Independent interaction matrix. In: IEEE Trans. on Robotics, Vol. 22, No. 4, pp.804-817.

Liu Y. H., Wang H., Chen W., and Zhou D. (2013) Adaptive visual servoing using common image features with unknown geometric parameters, Automatica, Vol. 49, No.8, pp.2453-2460.

Slotine J. J. and Li W. (1987). On the adaptive control of robot manipulators, Int. J. Robotics Research, Vol. 6, pp. 49-59.

Khalil H K(1996). Nonlinear Systems. Upper Saddle River, N. J.: Prentice Hall.

Simaan N., Taylor R. and Flint P. (2004). A dexterous system for laryngeal surgery, In: IEEE Conf. Robotics and Automation, pp. 351–357, New Orleans

Siciliano Bruno, Sciavicco Lorenzo, Villani Luigi, Oriolo Giuseppe (2009). Robotics Modelling, Planning and Control. Springer.

Tatlicioglu E., Walker D. (2007). Dynamic Modeling for Planar Extensible Continuum Robot Manipulators, In: Proc. IEEE Intl. Conf. on Robotics and Automation, pp. 1357–1362. Roma, Italy.

Trivedi D., Rahn C. D., Kier W. M., and Walker I. D. (2008). Soft robotics: Biological inspiration, state of the art, and future research. Applied Bionics and Biomechanics,5(3):99–117.,

Trivedi D, Lotfi A and Rahn C D(2008). Geometrically exact models for soft robotic manipulators. IEEE Trans. on Robotics, Vol. 24, pp. 773–80.

Wang H., Liu Y. H. and Zhou D.(2008). Adaptive visual servoing using point and line features with an uncalibrated eye-in-hand camera. IEEE Trans. on Robotics, Vol. 24, No. 4, pp. 843-857.

Wang H., Chen W. and Liu Y. H.(2012). Visual servoing of robots with uncalibrated robot and camera parameters. Mechatronics, Vol. 22, No. 4, pp. 390-397.

Wang H., Chen W., Yu X., Deng T., Wang X., and Pfeifer R. (2013). Visual Servo Control of Cable-driven Soft Robotic Manipulator. In: Prof. of IEEE Int. Conf. on Intelligent Robot and Systems, Tokyo, Japan.

Webster, Jones R.J., B.A.(2010). Design and Kinematic Modeling of Constant Curvature Continuum Robots: A Review. Robotics Research, Vol.29,No.13, pp.1661-1683

Wolf, Brown H. B., Casciola R., Costa A., Schwerin M., Shamas E. and Choset H. (2003). A mobile hyper redundant mechanism for search and rescue tasks. In: Proc. IEEE/RSJ Intl. Conf. on Intelligent Robots and Systems, Vol. 3, pp. 2889–2895, Las Vegas, Nevada

Zheng T., Branson D. T., Guglielmino E., and Caldwell D. G. (2011). A 3D Dynamic Model for Continuum Robots Inspired by An Octopus Arm. In: Prof. of IEEE Int. Conf. on Robotics and Automation, pp. 3652–3657, Shanghai,China.